Supplementary information

A – Tracking data summary

Table 1 - Description of tracked individuals, respective sampling rate, duration, start and end of monitoring period. Names with the same superscript alphabet letter indicate a couple (maned wolves take only one mate for life). No superscript alphabet letter indicates the absence of a mate in our data. Source: Adapted from de Paula (2016).

Name	*Sex*	*Weight (kg)*	*Age at first capture*	*Sampling rate (h)*	*Monitored days*	*GPS points*	*Start date*	*End date*
Amadeu[A]	M	29	6	1 - 6	461	3514	20/03/2007	20/10/2008
Lais[A]	F	31	6	0.4 - 6	433	3726	03/05/2007	28/07/2008
Bolt[B]	M	34	6	1	547	12917	01/10/2013	31/03/2015
Rose[B]	F	27	4	1	356	8527	20/07/2014	10/07/2015
Gamba[C]	M	30	6	4	98	562	30/04/2009	05/08/2009
Tay[C]	F	32	7	2	841	8760	14/03/2007	05/12/2009
Miro[D]	M	30	7	2 - 5	382	2687	25/03/2011	29/02/2012
Luna[D]	F	30	7	1	295	5775	28/02/2013	19/11/2013
Samurai[E]	M	32	4	4	86	496	26/08/2009	19/11/2009
Jurema[E]	F	28	3	4	510	2846	03/09/2009	25/01/2011
Henry	M	27	3	4	250	1451	12/05/2010	22/01/2011
Loba	F	27	3	3 - 11	563	2317	15/06/2012	29/12/2013
Nilde	F	27	7	2	59	618	30/03/2011	27/05/2011

B - Downsampling MODIS NDVI

We followed the methods described in Rao 2015 for disaggregation of each MODIS pixel to extract a fine spatial-temporal resolution NDVI time series (MF-NDVI). Despite the complex vegetation dynamics driving NDVI changes, short-term changes in NDVI values can be interpreted as linear (Rao et al. 2015):

$$NDVI_{t_{n+1}} = NDVI_{t_n} + k(t_{n+1} - t_n) \quad (1)$$

Here $NDVI_{t_{n+1}}$ is the NDVI value at the date t_n , $NDVI_{t_{n+1}}$ is the NDVI value at the date t_{n+1}, and k is the corresponding growth rate between t_{n+1} and t_n. This equation allows the prediction of NDVI on a given date by using the growth rate in that period and one NDVI observation as baseline.

The NDVI growth rate between any two dates can be calculated using MODIS NDVI time-series data. However, estimating NDVI growth rates for finer scale pixels from the growth

rate at the MODIS pixel is a more complex issue. For this we employed a linear mixing model (LMM) as proposed by (Rao et al. 2015):

$$NDVI(x,y,t) = \sum_{c=1}^{n} f_c(x,y,t) * NDVI_c(x,y,t) + \varepsilon(x,y,t) \quad (2)$$

Here $NDVI(x,y,t)$ is the NDVI value of a MODIS pixel (x,y) at time t, $f_c(x,y,t)$ and $NDVI_c(x,y,t)$ are respectively the fractional coverage and the NDVI value of land cover class c within the MODIS pixel (x,y) at time t ,n is the total number of the land cover classes within the MODIS pixel (x,y) and $\varepsilon(x,y,t)$ is the error introduced by LMM.

Considering Equation 1, Equation 2 and under the assumption that no land cover changes occur between t_1 and t_2, we can write the relationship between the growth rate of a MODIS pixel and the corresponding finer pixels as Equation 3.

$$k^{MODIS}(x,y,t_1 \rightarrow t_2) = \sum_{c=1}^{n} f_c(x,y,t_1) * k_c^{FINER}(x,y,t_1 \rightarrow t_2) \quad (3)$$

Here $k^{MODIS}(x,y,t_1 \rightarrow t_2)$ is the growth rate of a MODIS pixel (x,y) from t_1 to t_2, $k_c^{FINER}(x,y,t_1 \rightarrow t_2)$ is the growth rate of land cover c on the finer pixel scale within the corresponding MODIS pixel from t_1 to t_2 .

There are several land cover classes within a MODIS pixel (Figure 1), which means that the estimate of the unknown parameters, and therefore the computation of the finer scale NDVI growth rates, requires at least n MODIS pixels (Rao et al. 2015). These MODIS pixels are arranged in a system of equations, so that there are at least n equations to find the unknown parameters and the growth rate for each land cover type,

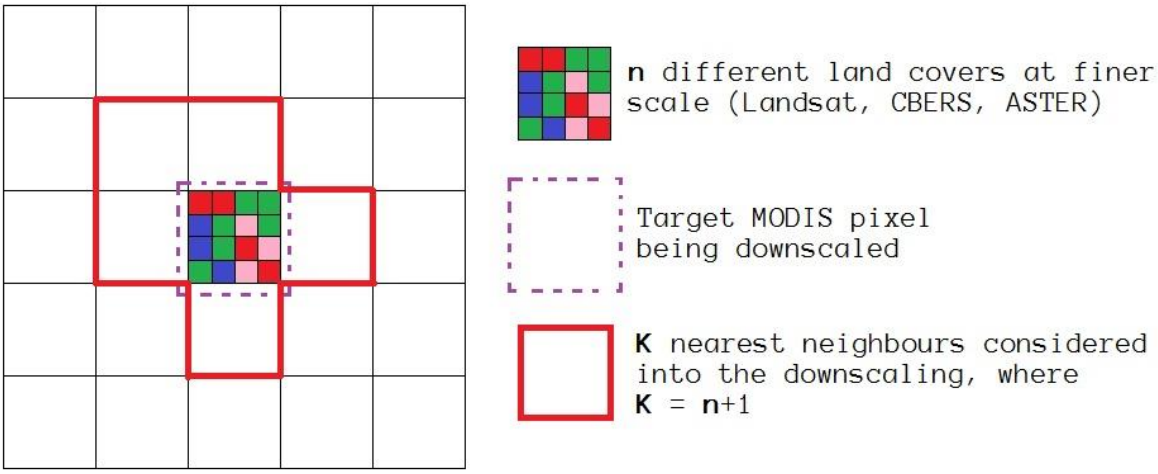

Figure 1 - The spatially neighbouring pixels of a target MODIS pixel being downscaled and land cover composition in a MODIS pixel classified from available LANDSAT, ASTER or CBERS images. The neighbourhood shape and size vary for each MODIS pixel being downscaled because it is determined by the number of land cover classes within the targeted MODIS pixel.

The estimate growth rates by land cover fractions are then computed by solving a linear system of $n+1$ equations, where each line expresses the combination of land covers and respective coarse NDVI growth rate for a MODIS pixel neighbouring the target MODIS pixel being downscaled (Figure 1). The neighbours for each downscale were selected by their centroid to centroid distance to the target pixel (Figure 1) and the system was solved using a constrained least square method with upper and lower boundaries, as per this:

$$k_{min}^{MODIS} - StD(k^{MODIS}) \leq k_c^{FINER} \leq k_{max}^{MODIS} + StD(k^{MODIS}) \quad (4)$$

Here $StD(k^{MODIS})$, k_{min}^{MODIS} and k_{max}^{MODIS} are the standard deviation, the minimum and the maximum values of the MODIS growth rate for the entire study area at the given date. The constraints are used to avoid unreasonable rates retrieved by Equation 4 that might be caused by classification errors and noise in the time-series (Rao et al. 2015).

Once the LMM is solved and the estimate growth rates of all land cover classes are calculated at the finer spatial scale, Equation 1 can be used to predict the finer NDVI value at t_2.

$$MF - NDVI_{t_{n+1}} = NDVI_{t_n}^{FINER} + k_n * (t_{n+1} - t_n) \quad (5)$$

Here $MF - NDVI_{t_{n+1}}$ is the spatially disaggregated NDVI value at the date t_n at the finer resolution, $NDVI_{t_{n+1}}^{FINER}$ is the NDVI value at the date t_{n+1} at the finer resolution image, and k_n is the corresponding growth rate between t_{n+1} and t_n for the land cover class n.

C – Suitability of MF-NDVI time series

As we did not have access to temporal ground-truthing data, we plotted the MF-NDVI time series to visualise if it was reporting the seasonal changes on vegetation in a reasonable manner. For this we selected pixels from areas where the multi-temporal land cover classification by (de Paula 2016)indicated a specific crop type instead of a generic "farmland" area. The reason for this choice is that the knowledge of the crop type allows the comparison between the agricultural calendar (harvest, plating, growing) for that specific crop in that region and the MF-NDVI values. The only specified crop in the area was coffee fields, which have well defined seasons.

The average MF-NDVI time series from three pixels from different coffee crops is shown in Figure 2, the time axis covers the same period for which we had a verified land cover map. The knowledge of the land cover allowed us to compare the MF-NDVI curve to the expected NDVI pattern for that specific land cover, considering dry and rainy seasons or harvesting and planting seasons. In addition to being the only specified farmland, coffee crops have a well-known NDVI signature which has been used for mapping coffee fields in Brazil (Alves et al. 2016; Bernardes et al. 2012) and allowed us to check if our MF-NDVI product was in accordance with the land cover dynamics.

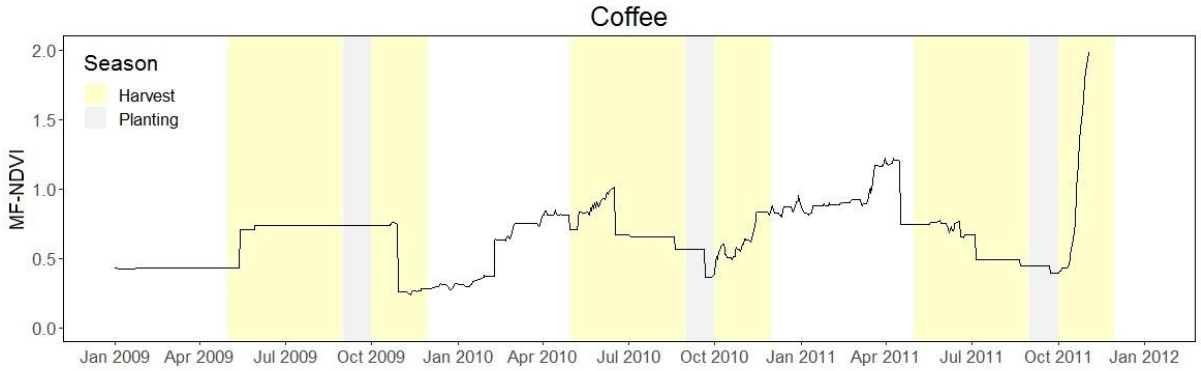

Figure 2 - Average MF-NDVI time series from three pixels from different coffee crops, the time axis covers the

same period for which we had a verified land cover map. The crop seasons are shown by background colours explained in the legend.

The MF-NDVI was able to capture the seasonal variations in the phenology of the coffee crops. As expected, the lower values are found around the planting season, which is coherent with the field being bare soil during that period and therefore having the lowest MF-NDVI responses. The highest MF-NDVIs are found immediately before the harvest season, reflecting the productive peak of the plant. There is a spike in MF-NDVI values after October 2011, which is a result of the lack of higher resolution images between August 2011 and July 2012, a result of malfunctioning of the Landsat 5 and 7 satellites during that period. This indicates a high sensitivity of the model to the absence of higher resolution images. Therefore, a series of higher resolution NDVI images spread evenly across the study period is preferred and more likely to produce more accurate MF-NDVI.

Despite this sensitivity to the lack of high-resolution images, the MF-NDVI preserved the seasonal trends, i.e., seasonal changes were still preserved even where absolute values were not as accurate. Since the changes and trends are more relevant for our study than the absolute values of MF-NDVI, as they give us information on the dynamics of the landscape in which maned wolves were moving, this did not pose a particular problem.

References

Alves, H. M. R., M. M. L. Volpato, T. G. C. Vieira, D. A. Maciel, T. G. Gonçalves, and M. F. Dantas. 2016. "Characterization and Spectral Monitoring of Coffee Lands in Brazil." *ISPRS - International Archives of the Photogrammetry, Remote Sensing and Spatial Information Sciences* XLI-B8 (June): 801–3. https://doi.org/10.5194/isprsarchives-XLI-B8-801-2016.

Bernardes, Tiago, Mauricio Alves Moreira, Marcos Adami, and Bernardo Friedrich Theodor Rudorff. 2012. "Monitoring Biennial Bearing Effect on Coffee Yield Using MODIS Remote Sensing Imagery." *International Geoscience and Remote Sensing Symposium (IGARSS)*, no. August: 3760–63. https://doi.org/10.1109/IGARSS.2012.6350499.

Paula, Rogério C. de. 2016. "Adequabilidade Ambiental Dos Biomas Brasileiros à Ocorrência Do Lobo-Guará (Chrysocyon Brachyurus) e Efeitos Da Composição Da Paisagem Em Sua Ecologia Espacial, Atividade e Movimentação." University of São Paulo. http://www.teses.usp.br/teses/disponiveis/11/11150/tde-05072016-114911/pt-br.php.

Rao, Yuhan, Xiaolin Zhu, Jin Chen, and Jianmin Wang. 2015. "An Improved Method for Producing High Spatial-Resolution NDVI Time Series Datasets with Multi-Temporal MODIS NDVI Data and Landsat TM/ETM+ Images." *Remote Sensing* 7 (6): 7865–91. https://doi.org/10.3390/rs70607865.